Kashf Journal of Multidisciplinary Research
Vol: 03 – Issue 04 (2026)
P-ISSN: 3007-1992
E-ISSN: 3007-200X
https://kjmr.com.pk

Stress Relaxation Kinetics and Post-Deformation Microstructural Features in Aged Aluminum Alloy AA6061

S. Tabinda Munib
M.Phil. Research Scholar, School of Physics Minhaj University Lahore
Email: *shehrzadee@gmail.com*

Hafsa Iftikhar
M.Phil. Scholar Minhaj University Lahore
Email: *hafsasaqib1729@gmail.com*

Faiza Yousaf
Department of Physics, UET Lahore.
Email: *faizayousaf621@gmail.com*

****Corresponding Author :***(*hafsasaqib1729@gmail.com*)

DOI: *(https://doi.org/10.71146/kjmr884)*

Article Info

Abstract

The Stress relaxation behavior of Aluminum 6061 alloy artificially aged at 200°C for different time intervals was examined using Tensile Testing Machine at a constant strain rate.The Stress Relaxation rates was determined at strain intervals of about 0.5% until fracture.It was found that stress relaxation curves were logarithmic, except at large 't' when they flattened .The stress relaxation rate was found to increase with initial stress levels and aging time upto 6hr, while the 8hr-aged sample exhibited a decline in stress relaxation rate.Similarly activation energy for stress relaxation increased from 0.85eV to 1.46eV upto 6hr of aging and decreased from 1.46eV to 1.29eV in the overaged specimen.A progressive increase in activation energy correlates with fractograph analysis using SEM.The Variations in stress relaxation rates and activation energy in the case of aged and overaged specimens were due to changes in slip processes responsible for work hardening. SEM fractographs showed a transition from ductile dimple fracture in unaged samples to a brittle fracture mode in over-aged specimens. These results highlight the critical role of microstructural evolution in dictating the stress relaxation behavior of AA6061 alloy, providing valuable insights into optimizing its performance in applicatons where long term mechanical stability is required.

Keywords:
Aging Heat Treatment, XRF, Stress Relaxation, Activation Energy, SEM, Microsturcture Fractograph Analysis

1. Introduction

Aluminum alloys, particularly the 6xxx series, have emerged as indispensable materials in aerospace, automotive, and structural applications due to their remarkable strength-to-weight ratio, corrosion resistance, and weld ability [1, 2]. Among these, AA6061 is prominently utilized owing to its superior mechanical properties and formability, which can be further enhanced through artificial aging treatments [3,4]. Nonetheless, during processing and service, these alloys frequently encounter residual stresses that can profoundly impact their long-term performance and dimensional stability [5,6]. The implications of artificial aging on stress relaxation constitute a significant concern, as it can profoundly influence dislocation dynamics and recovery mechanisms within the alloy matrix [7,8]. While aged alloys are anticipated to demonstrate distinctive stress-relaxation behaviors attributable to the stabilization of precipitate structures, their unaged counterparts may exhibit expedited relaxation due to enhanced dislocation mobility [9,10]. The mechanical behavior of AA6061 exhibits a pronounced sensitivity to thermal treatments, notably aging, which profoundly impacts its microstructure and the relaxation behavior of residual stresses [1,2,10,14]. Artificial aging augments mechanical properties through the mechanism of precipitation hardening, predominantly characterized by the formation of Mg_2Si phases [20,25]. Nevertheless, the responses of aged and unaged conditions to stress relaxation diverge significantly, particularly under varying strain rates and thermal environments [1,21]. Stress relaxation, a time-dependent diminution of stress under constant strain, is pivotal in determining the long-term dimensional stability and fatigue life of aluminum components [14, 21]. Prior investigations have elucidated that aging not only modifies the yield strength and hardness but also influences the alloy's capacity to dissipate internal stresses over time [2, 25]. Moreover, factors such as pre-straining, dislocation density, and residual microstructural stresses significantly govern the relaxation behavior [15, 27]. This study endeavors to systematically examine the stress relaxation behavior of both aged and unaged AA6061 under meticulously controlled conditions. By scrutinizing mechanical responses and microstructural alterations, it aims to elucidate the mechanisms underpinning stress relaxation and provide valuable insights for enhanced processing strategies and life prediction models.

2. EXPERIMENTAL WORK

Aluminum Alloy (AA6061) in the form of plate was obtained from commercial market. The chemical composition observed using X-ray Flourescence Analysis (XRF) revealed that Al-Mg-Si Alloy was composed of Al (97.07%), Mg (1.24%), Si (0.67%) and Fe (0.53%) . The samples in the form of strips having dimension 8 cm × 8 mm × 4 mm were cut from the as received sheet using a Computerized Numerical Control (CNC) wire-cutting machine. For

microstructural analysis, the specimens were metallographically prepared by grinding with silicon carbide abrasive papers of grit sizes ranging from 150 to 4000 on a Struers Knuth rotor machine, followed by polishing with diamond paste (1–3 µm).The polished specimens were given solution heat treatment at 440 °C for 1 hour in a muffle furnace, followed by a rapid water quenching using distilled water to form a supersaturated solid solution. Artificial aging was carried out at a constant temperature of 200°C for different durations of 0 , 2, 4, 6, and 8 hours to study the evolution of microstructure and influence of aging on mechanical behavior of the alloy. Stress relaxation measurements were taken using a Universal Testing Machine. The deformation was recorded by the linked computer in the form of stress-strain curves. Each sample experienced a constant deformation rate of 3.3×10^{-4} mm/s for 30 seconds, followed by a relaxation period of 60 seconds. This cycle was repeated 10 times to gather reliable stress relaxation data under different aging conditions.The surface morphology of the solution treated and aged specimens was examined using scanning electron microscope (SEM).

3. RESULTS & DISCUSSION

3.1 Mechanical Tests

To assess the mechanical properties of each sample, tensile tests were coducted using Universal Testing Machine (UTM) and the stress-relaxation data was collected. The deformation behavior of each specimen at the given temperature was characterized by a series of stress levels σ0 , at which straining was interrupted. The stress relaxation curves corresponding to these specimens are presented in Figures 3.1 to 3.5. The results reveal that the Srel values increase with longer aging times at 200°C, suggesting that the alloy's response to stress relaxation becomes more pronounced with increased aging.

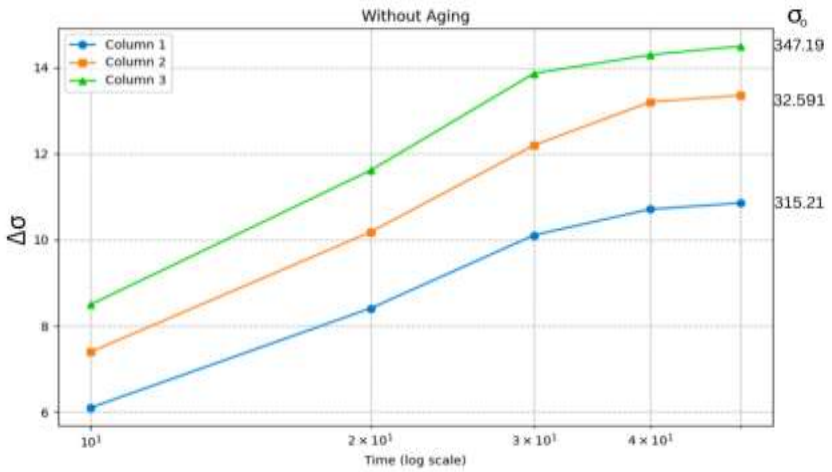

Figure 3.1 Alloy's Response to Stress Relaxation without Aging

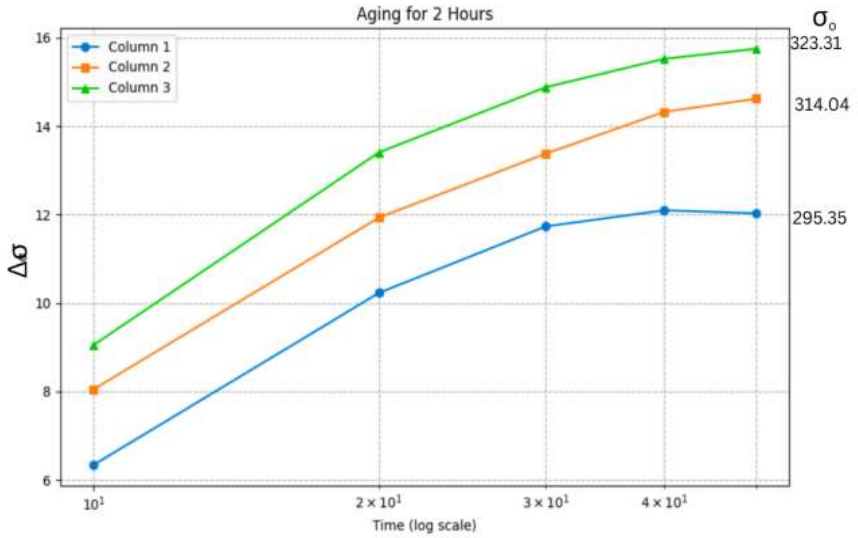

Figure 3.2 Alloy's Response to Stress Relaxation with 2 Hours of Aging

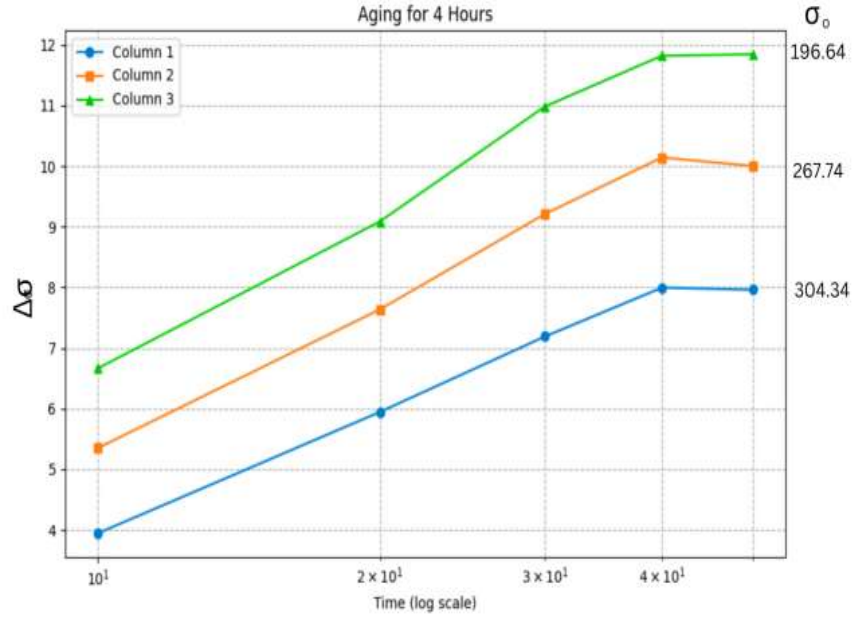

Figure 3.3 Alloy's response to stress relaxation with 4 Hours of Aging

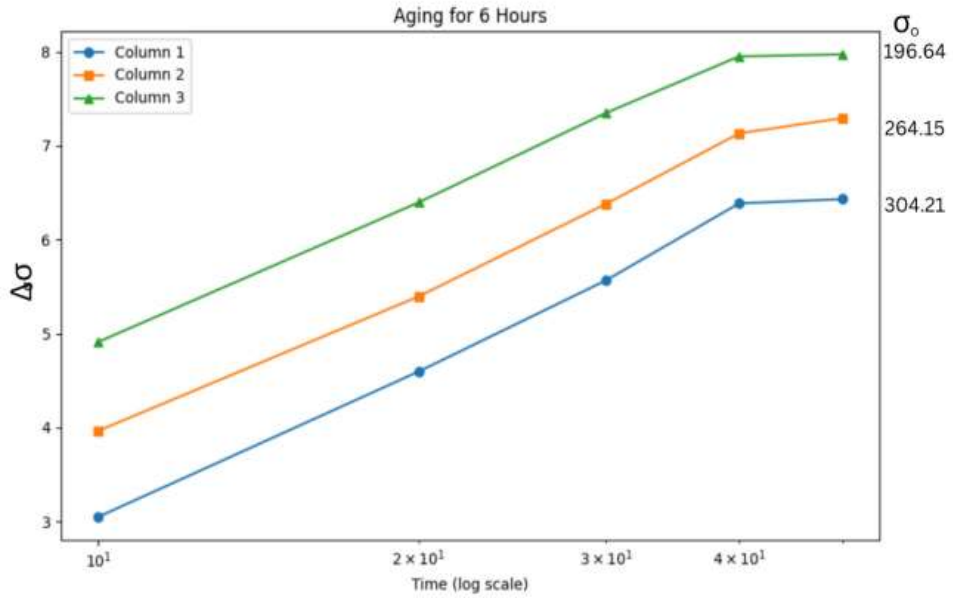

Figure 3.4 Alloy's Response to Stress Relaxation with 6 Hours of Aging.

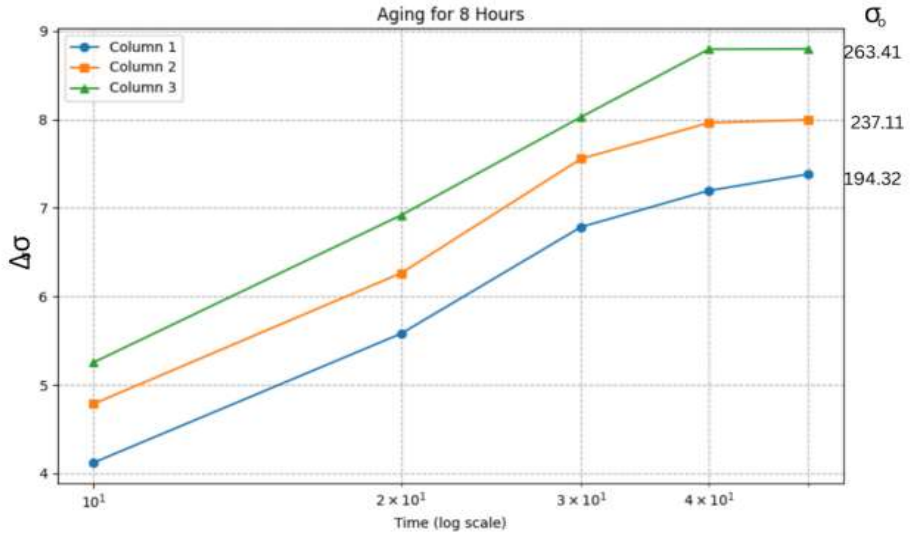

Figure 3.5 Alloy's Response to Stress Relaxation with 8 Hours of Aging

3.2 Stress Relaxation Results

The stress relaxation curves demonstrated a logarithmic pattern, with the rates of stress reduction exhibiting a gradual flattening over time, signifying diminished relaxation rates as aging progressed. This observation aligns with the simple Stochastic Model of Creep and Stress Relaxation in solids proposed by Feltham. He showed that the logarithmic form of creep is more adequately presented by the relation

$$\varepsilon = \text{Scr} \log(1+t/t01)/(1+t/t02),\ t01 < t02 \quad \text{----------} \quad (1)$$

Where Scr is the creep coefficient and t01 and t02 are retardation times associated with the activation process. For shorter times , this relation simplifies to:

$$\varepsilon = \text{Scr} \log(1+ t/to) \text{ ----------} (2)$$

Thee above equation is indicating that strain increases logarithmically with time.

For stress relaxation at constant strain, the corresponding form can be expressed as:

$$-\Delta\sigma = \text{Srel} \log(1+ t/to) \text{ ----------} (3)$$

Here $\Delta\sigma = \sigma0(\varepsilon) - \sigma(t, \varepsilon)$,where $\sigma0(\varepsilon)$ is the stress at the onset of the relaxation. This relation signifies that the decrease in stress with time is logarithmic, consistent with experimental observations.The slope is time-dependent and is given by,

$$\text{Srel} = d\sigma0 / d \log (1+ t/to) \text{ ----------} (4)$$

To assess the activation energy associated with the stress relaxation process, the derivative of the stress-relaxation slope, dSrel/dσo, was measured for each sample. Under theoretical conditions, it is expected that stress relaxation would be zero when no stress is applied. However, due to limitations in the measurement equipment, accurate data could not be obtained at lower stress levels. Consequently, the extrapolated curves may exhibit non-linearity at these lower stress levels. Samples subjected to prolonged aging (up to 6 hours) exhibited an enhanced resistance to stress relaxation, whereas the 8-hour sample manifested a decline as shown in fig 3.6.

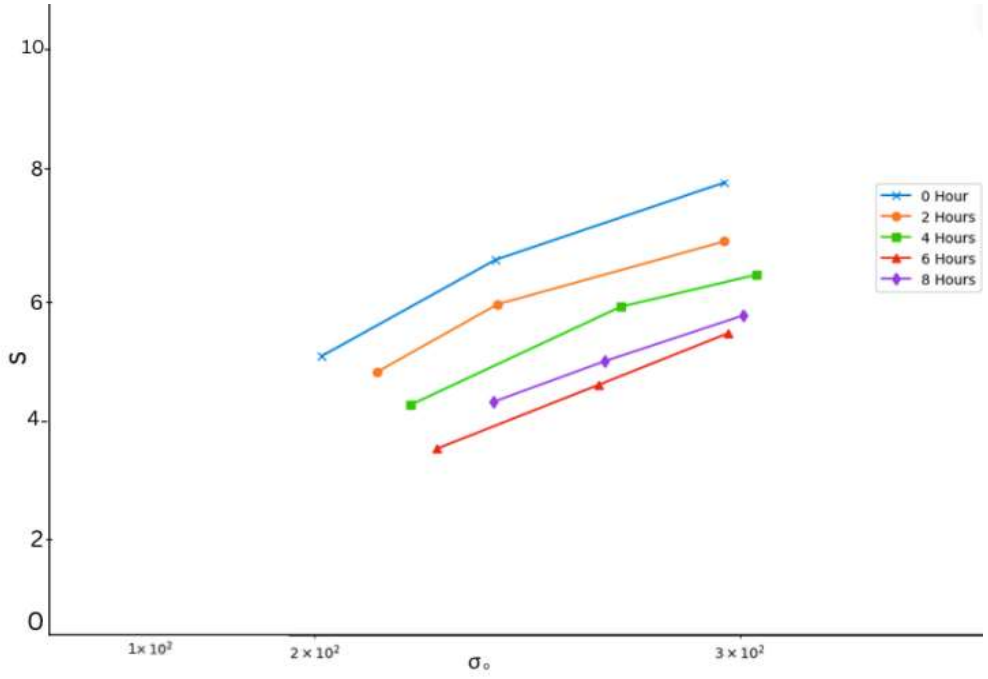

Figure 3.6 Srel Vs σ0 curves

The stress relaxation (Srel) decreases with increasing aging time from 0 to 6 hours, indicating a reduction in stress relaxation rate as shown in the fig 3.7. During the aging process, fine Mg_2Si precipitates form and strengthen the Al 6061 alloy through precipitation hardening. This microstructural evolution restricts dislocation movement, increasing the activation energy required for relaxation. Consequently, aged samples exhibit slower stress relaxation compared to unaged ones. Initially, at 0 hours, the alloy is softer and relaxes stress rapidly, while at prolonged aging (6hours), the alloy becomes harder and more thermally stable, leading to a lower relaxation rate and greater mechanical stability.

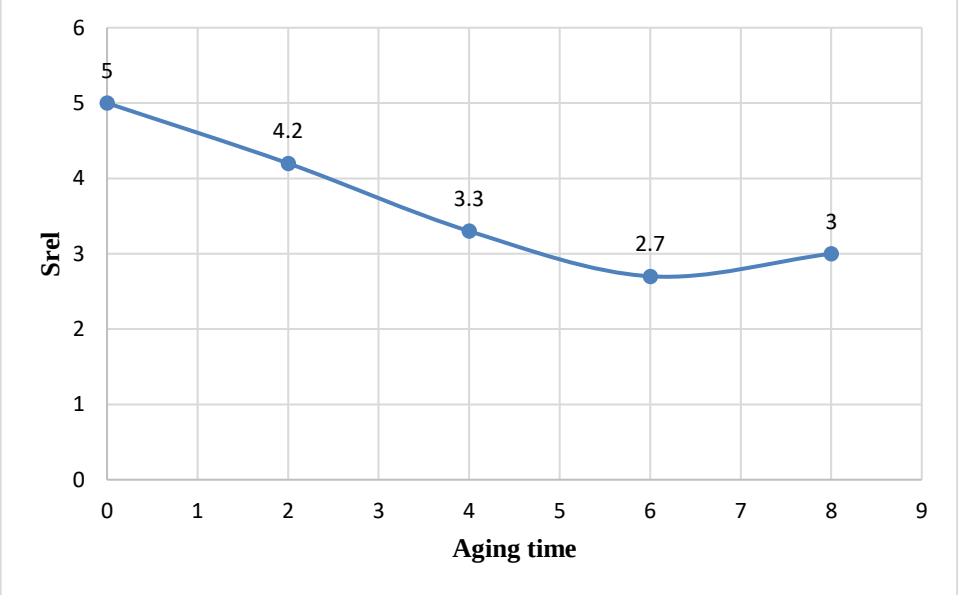

Figure 3.7 Srel Vs Aging time

At prolonged aging time (8 hours), the Al 6061 alloy entered the overaged condition, where the fine strengthening precipitates (Mg_2Si) began to coarsen and lose their effectiveness in hindering dislocation movement. This coarsening reduced the density of coherent precipitates, lowering the alloy's strength and hardness. As a result, dislocations moved more freely , leading to an increase in stress relaxation compared to the peak-aged condition (e.g., 6 hours). Therefore, while stress relaxation generally decreased with aging time, an increase at extended aging (overaging) is justified by the precipitate coarsening and reduced activation energy, which reactivates relaxation mechanisms in the alloy.

3.3 Activation Energy

The activation energy for stress relaxation was determined by the relation given by the equation ,

$$dSrel / d\sigma o = U0/kT \, . \, 1/ \sigma o \quad \text{---------- (5)}$$

Where,

$$U0 = kT \, . \, (d\sigma 0 / dSrel) + m \quad \text{---------- (6)}$$

Substituting the value of K= 0.8617×10^{-4} eV/ K^{-1} , T= 295K and m= 25, the activation energies for 0, 2, 4, 6 and 8 hours were calculated using equation (6) as 0.85eV, 1.07eV,

1.24eV ,1.46eV,1.29eV.The progressive increase in activation energy up to 6 hours was positively correlated with the formation of fine Mg_2Si precipitates, which obstructed dislocation motion. Conversely, the reduction observed at 8 hours was ascribed to the coarsening of precipitates (Ostwald ripening), thereby reducing their efficacy.

Time (hours)	Activation Energy (eV)
0	0.85
2	1.07
4	1.24
6	1..46
8	1.29

Table 3.1 Activation Energy Vs Time

These values of activation energies suggest how the energy required for stress relaxation varies with the aging time of the alloy.The plot of Activation energy and aging time is given below.

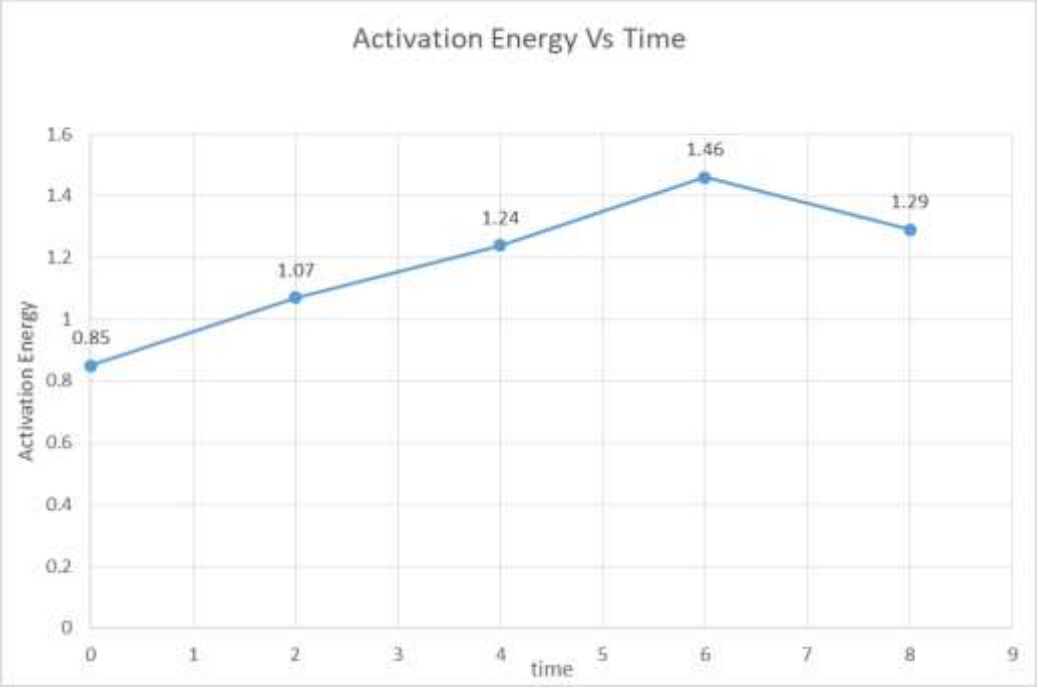

Figure 3.8 Activation Energy Vs Aging Time

3.4 Fractograph Analysis

The Fractograph analysis was carried using Scanning Electron Microscopy (SEM). The results revealed clear distinctions between unaged and aged Aluminum Alloy 6061 samples. The unaged sample exhibited well-defined, deep dimples on the fracture surface, characteristic of a ductile fracture mechanism. With progressive aging, these dimples became shallower and more flattened, indicating a shift toward a moderately ductile fracture mode due to changes in the microstructure. Notably, the sample aged for 6 hours showed an optimal distribution of fine Mg_2Si precipitates, resulting in the highest resistance to stress relaxation and a peak activation energy of 1.46 eV. This optimal aging condition effectively impeded dislocation motion, enhancing the mechanical strength of the alloy. However, at 8 hours of aging, signs of over-aging were evident, with SEM images revealing coarser precipitates attributed to Ostwald ripening. This coarsening reduced the effectiveness of dislocation pinning, thereby lowering both the activation energy (U_0) and the mechanical properties of the alloy. The microstructural evolution observed through SEM highlights the strong correlation between aging time, precipitate size, and fracture behavior. While the findings are consistent with known mechanisms of precipitation hardening, they provide new insights into how stress relaxation kinetics are influenced by microstructural changes during the aging process. These findings align with prior studies on precipitation hardening but provide novel insights into the role of stress relaxation kinetics during aging.

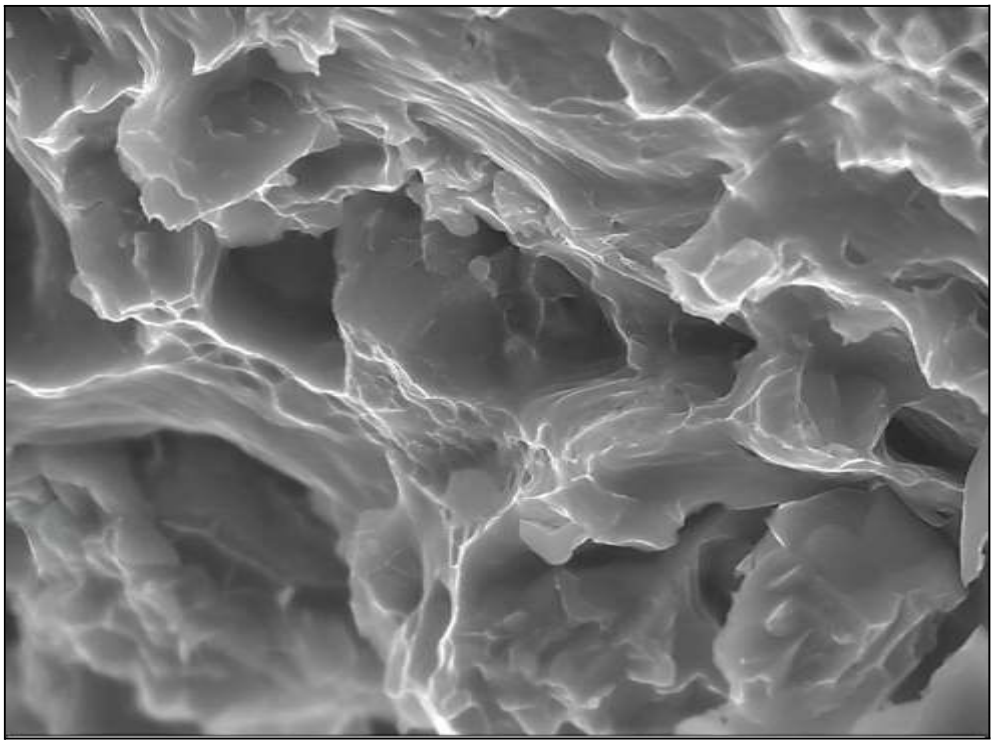

Figure 3.9 SEM Micrograph (Meg = 5KX) of Unaged Al-Alloy (6061)

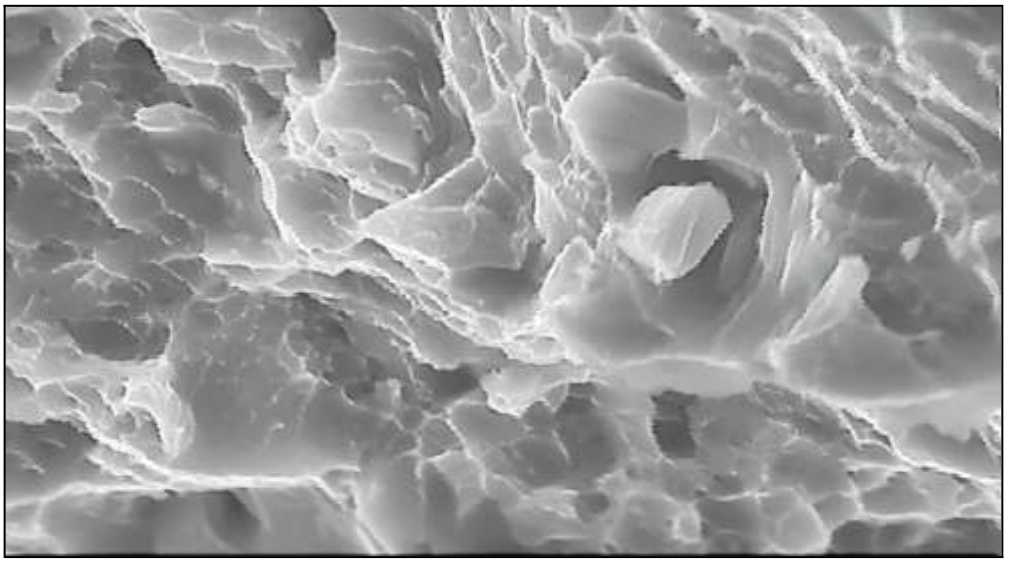

Fig 3.10 SEM Micrograph (Meg = 5KX) of Al-Alloy (6061) of Aging for 2 Hours

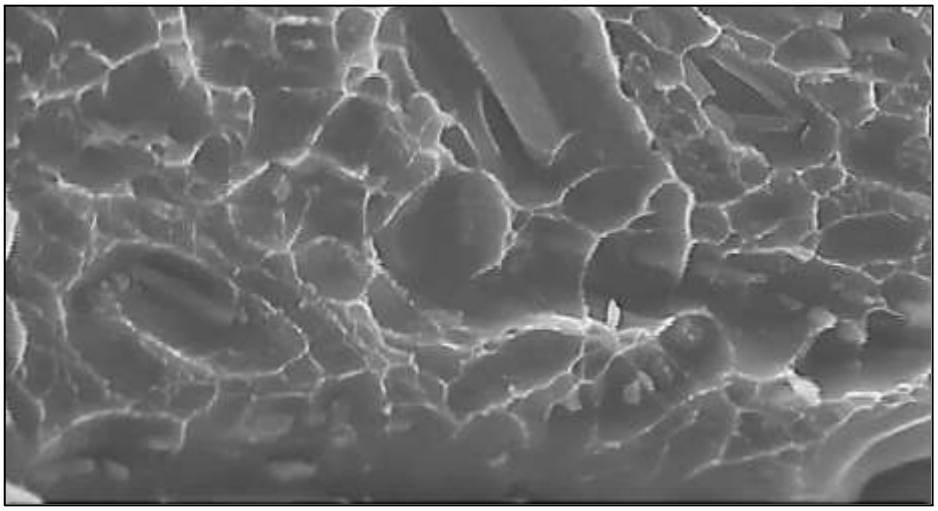

Figure 3. 11 SEM Micrograph (Meg = 5KX) of Al-Alloy (6061) of Aging for 4 Hours

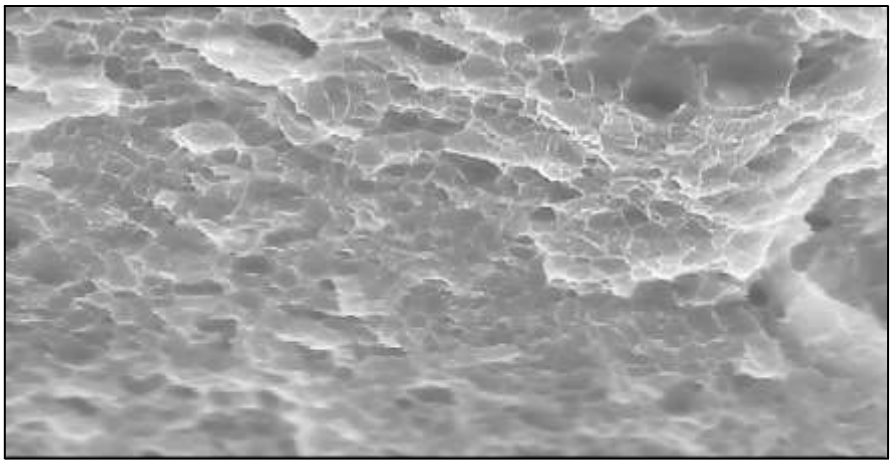

Figure 3. 12 SEM Micrograph (Meg = 5KX) of Al-Alloy (6061) of Aging for 6 Hours

Figure 3. 13 SEM Micrograph (Meg = 5KX) of Al-Alloy (6061) of Aging for 8 Hours

4. CONCLUSIONS

1. Stress relaxation behavior of Al 6061 is significantly influenced by aging time, with distinct changes in microstructure and mechanical response observed at different durations.

2. Peak aging was achieved at 6 hours at 390°F, where finely dispersed Mg_2Si precipitates were observed. This condition provided the highest resistance to stress relaxation and maximum activation energy of 1.46 eV.

3. Unaged samples showed a ductile fracture mode, while aging led to a transition toward moderately ductile fracture due to microstructural evolution.

4. Over-aging at 8 hours resulted in coarser precipitates due to Ostwald ripening, which reduced dislocation pinning, mechanical strength, and stress relaxation resistance.

5. The study highlights a strong correlation between aging time, precipitate morphology, and fracture behavior, as confirmed by SEM micrographs.

6. The findings can be used to optimize aging parameters for Al 6061, balancing strength, ductility, and stress relaxation resistance for targeted industrial applications.

REFERENCES

Adesola, A., Odeshi, A., & Lanke, U. (2013). The effects of aging treatment and strain rates on damage evolution in AA 6061 aluminum alloy in compression. *Materials & Design*, *45*(7), 212–221.

Ahmad, A., Afzal, N., & Rafique, M. (2021). Structural and mechanical response of artificially aged aluminum alloy 6061. *Strength of Materials*, *53*(3), 502–510.

Ayer, V. M., Miguez, S., & Toby, B. H. (2014). Why scientists should learn to program in Python. *Powder Diffraction*, *29*(2), 48–64.

Azarniya, A., Taheri, A. K., & Taheri, K. K. (2019). Recent advances in ageing of 7xxx series aluminum alloys: A physical metallurgy perspective. *Journal of Alloys and Compounds*, *781*(1), 945–983.

Budak, S., Çolak, H., & Yakut, Y. (2022). Effect of aging time and temperature on microstructure and mechanical properties of AA7075 alloy. *Gümüşhane Üniversitesi Fen Bilimleri Enstitüsü Dergisi*, *80*(7), 101-104.

Çam, G., & İpekoğlu, G. (2016). Recent developments in joining of aluminum alloys. *The International Journal of Advanced Manufacturing Technology*, *91*(8), 1851–1866.

Cao, X., & Campbell, J. (2005). Oxide inclusion defects in Al-Si-MG cast alloy. *Canadian Metallurgical Quarterly*, *44*(4), 435–448.

Carlberg, T., Bayat, N., & Erdegren, M. (2015). Surface segregation and surface defect formation during aluminum billet casting. *Transactions of the Indian Institute of Metals*, *68*(6), 1065–1069.

De Bonfils-Lahovary, M., Josse, C., Laffont, L., & Blanc, C. (2019). Influence of hydrogen on the propagation of intergranular corrosion defects in 2024 aluminium alloy. *Corrosion Science*, *148*(18), 198–205.

Demir, H., & Gündüz, S. (2009). The effects of aging on machinability of 6061 aluminium alloy. *Materials & Design*, *30*(5), 1480–1483.

Elhajjar, R., Law, C., & Pegoretti, A. (2018). Magnetostrictive polymer composites: Recent advances in materials, structures, and properties. *Progress in Materials Science*, *97*(8), 204–229.

El-Sayed, M. A., Hassanin, H., & Essa, K. (2016). Bifilm defects and porosity in Al Cast alloys. *The International Journal of Advanced Manufacturing Technology*, *86*(8), 1173–1179.

Gardi, R. H., Kadauw, A., & Hanschel, B. (2023). Effect of exfoliation corrosion on the mechanical properties of friction stir spot welded 2024-T3 AA joints. *Advances in Materials Science and Engineering*, *202*(3), 1–10.

Godlewski, L. A., Su, X., Pollock, T. M., & Allison, J. E. (2013). The effect of aging on the relaxation of residual stress in cast aluminum. *Metallurgical and Materials Transactions A*, *44*(10), 4809–4818.

Hao, H., Ye, D., Chen, Y., Feng, M., & Liu, J. (2015). A study on the mean stress relaxation behavior of 2124-T851 aluminum alloy during low-cycle fatigue at different strain ratios. *Materials & Design* ,*67*(5), 272–279.

Harris, Charles R., K. Jarrod Millman, Stéfan J. Van Der Walt, Ralf Gommers, Pauli (2020). "Array Programming With NumPy." *Nature 585(*7825), 357–362.

Hu, Y., Lin, X., Zhang, S., Jiang, Y., Lu, X., Yang, H., & Huang, W. (2018). Effect of solution heat treatment on the microstructure and mechanical properties of Inconel 625 superalloy fabricated by laser solid forming. *Journal of Alloys and Compounds*, *767*(7), 330–344.

Isadare, A. D., Aremo, B., Adeoye, M. O., Olawale, O. J., & Shittu, M. D. (2012). Effect of heat treatment on some mechanical properties of 7075 aluminium alloy. *Materials Research, 16*(1), 190–194.

Kumar, N. S., Dhruthi, N., Pramod, G., Samrat, P., & Sadashiva, M. (2022). A Critical review on heat treatment of aluminium alloys. *Materials Today, 58*(23), 71–79.

Kumar, M., Baloch, M. M., Abro, M. I., Memon, S. A., & Chandio, A. D. (2019). Effect of artificial aging temperature on mechanical properties of 6061 aluminum alloy. *Mehran University Research Journal of Engineering & Technology, 38*(1), 31-36.

Li, Y., & Shi, Z. (2022). A new method to characterize and model Stress-Relaxation aging behavior of aluminum alloys under age forming conditions. *Metallurgical and Materials Transactions A, 53*(4), 1345–1360.

Long, M., Jiang, F., Wu, F., Wu, M., & Su, Y. (2024). Effect of pre-strain on microstructure and corrosion behavior of a novel High-ZN containing AL-ZN-MG-CU alloy. *Journal of Materials Engineering and Performance, 234*(10), 1343-1348.

Nes, E., Marthinsen, K., & Rønning, B. (2001). Modeling the evolution in microstructure and properties during processing of aluminium alloys. *Journal of Materials Processing Technology, 117*(3), 333–340.

Opprecht, M., Garandet, J., Roux, G., Flament, C., & Soulier, M. (2020). A solution to the hot cracking problem for aluminium alloys manufactured by laser beam melting. *Acta Materialia, 197*(67), 40–53.

Ozturk, F., Sisman, A., Toros, S., Kilic, S., & Picu, R. (2010). Influence of aging treatment on mechanical properties of 6061 aluminum alloy. *Materials & Design 31*(2), 972–975.

26. Peng, D., Shen, J., Tang, Q., Wu, C., & Zhou, Y. (2013). Effects of aging treatment and heat input on the microstructures and mechanical properties of TIG-welded 6061-T6 alloy joints. *International Journal of Minerals Metallurgy and Materials, 20*(3), 259– 265.

Rajak, D. K., Kumaraswamidhas, L., Das, S., & Kumaran, S. S. (2016). Characterization and analysis of compression load behaviour of aluminium alloy foam under the diverse strain rate. *Journal of Alloys and Compounds, 656*(7), 218–22